Factors Influencing Short-term Synaptic Plasticity in the Avian Cochlear Nucleus Magnocellularis

Libertas Academica
FREEDOM TO RESEARCH

Supplementary Issue: Molecular and Cellular Mechanisms of Neurodegeneration

Jason Tait Sanchez[1,2], Karla Quinones[1,*] and Sebastian Otto-Meyer[3,†]

[1]Roxelyn and Richard Pepper Department of Communication Sciences and Disorders, The Hugh Knowles Hearing Research Center, School of Communication, Northwestern University, Evanston, IL, USA. [2]Department of Neurobiology and Interdepartmental Neuroscience Program, Northwestern University, Evanston, IL, USA. [3]Weinberg College of Arts and Sciences, Northwestern University, Evanston, IL, USA. *Current address: Children's Hospital of Wisconsin, Milwaukee, WI, USA. †Auditory Neuroscience Laboratory, Communication Sciences and Disorders, Northwestern University, Evanston, IL, USA.

ABSTRACT: Defined as reduced neural responses during high rates of activity, synaptic depression is a form of short-term plasticity important for the temporal filtering of sound. In the avian cochlear nucleus magnocellularis (NM), an auditory brainstem structure, mechanisms regulating short-term synaptic depression include pre-, post-, and extrasynaptic factors. Using varied paired-pulse stimulus intervals, we found that the time course of synaptic depression lasts up to four seconds at late-developing NM synapses. Synaptic depression was largely reliant on exogenous Ca^{2+}-dependent probability of presynaptic neurotransmitter release, and to a lesser extent, on the desensitization of postsynaptic α-amino-3-hydroxy-5-methyl-4-isoxazolepropionic acid-type glutamate receptor (AMPA-R). Interestingly, although extrasynaptic glutamate clearance did not play a significant role in regulating synaptic depression, blocking glutamate clearance at early-developing synapses altered synaptic dynamics, changing responses from depression to facilitation. These results suggest a developmental shift in the relative reliance on pre-, post-, and extrasynaptic factors in regulating short-term synaptic plasticity in NM.

KEYWORDS: AMPA receptors, desensitization, development, glutamate transporters, nucleus magnocellularis, short-term synaptic depression

SUPPLEMENT: Molecular and Cellular Mechanisms of Neurodegeneration

CITATION: Sanchez et al. Factors Influencing Short-term Synaptic Plasticity in the Avian Cochlear Nucleus Magnocellularis. *Journal of Experimental Neuroscience* 2015:9(S2) 11–24 doi:10.4137/JEN.S25472.

TYPE: Original Research

RECEIVED: August 7, 2015. **RESUBMITTED:** September 20, 2015. **ACCEPTED FOR PUBLICATION:** September 21, 2015.

ACADEMIC EDITOR: Lora Talley Watts, Editor in Chief

PEER REVIEW: Four peer reviewers contributed to the peer review report. Reviewers' reports totaled 1,092 words, excluding any confidential comments to the academic editor.

FUNDING: This work was supported by a National Research Service Award F32 DC010307 (JTS) from the National Institute on Deafness and Other Communication Disorders of the U.S. Public Health Service and by the Hugh Knowles Hearing Research Center and the School of Communication, Northwestern University. The authors confirm that the funder had no influence over the study design, content of the article, or selection of this journal.

COMPETING INTERESTS: Authors disclose no potential conflicts of interest.

CORRESPONDENCE: jason.sanchez@northwestern.edu

Paper subject to independent expert blind peer review. All editorial decisions made by independent academic editor. Upon submission manuscript was subject to anti-plagiarism scanning. Prior to publication all authors have given signed confirmation of agreement to article publication and compliance with all applicable ethical and legal requirements, including the accuracy of author and contributor information, disclosure of competing interests and funding sources, compliance with ethical requirements relating to human and animal study participants, and compliance with any copyright requirements of third parties. This journal is a member of the Committee on Publication Ethics (COPE).

Published by Libertas Academica. Learn more about this journal.

Introduction

Synaptic dynamics are an essential part of information processing between neurons in the central nervous system.[1] In the auditory brainstem, short-term synaptic depression plays an important computational role in sound processing of normal and hearing-impaired individuals.[2] Defined as reduced neural responses during high rates of activity, short-term synaptic depression is an excellent example of temporal filtering critical for encoding cues used for sound localization and signal discrimination.[3,4] Studies from multiple brain regions have demonstrated that mechanisms underlying short-term synaptic depression include pre-, post-, and extrasynaptic factors.[5] The purpose of this study was to determine the extent to which similar factors give rise to short-term synaptic depression at two functionally distinct developmental time periods in the avian cochlear nucleus magnocellularis (NM), a first-order auditory brainstem synapse.

Presynaptic terminals influence the firing of postsynaptic neurons by releasing different amounts of neurotransmitter in an activity-dependent manner.[6] When separated by only tens of milliseconds, repetitive action potential (AP) arrival at presynaptic terminals can transiently deplete the readily releasable pool of neurotransmitter and correspondingly decrease the response of its postsynaptic target.[7] This reduction in synaptic strength can last for hundreds of milliseconds to seconds.[8] Other presynaptic factors that account for short-term synaptic depression include the inactivation of neurotransmitter release sites and a decrease in exogenous calcium influx.[9–11] Short-term synaptic depression can also occur though desensitization of postsynaptic AMPA-type glutamate receptors (AMPA-Rs).[12–19] Although the release of neurotransmitter immediately activates postsynaptic AMPA-Rs during periods of repetitive activity, a majority of these receptors become nonresponsive to the ligand overtime (ie, desensitized) and can take several seconds before recovering from their desensitized state.[20] Finally, because of their close proximity to pre- and postcomponents of the synapse, glutamate transporters have an established role in regulating

the speed and amount of neurotransmitter clearance from the synaptic cleft.[21] As such, extrasynaptic factors mediated by glutamate transporters located on glial and neural cells might play an additional role in regulating short-term synaptic depression by impacting the degree of postsynaptic AMPA-R activation and desensitization.[22–24] Taken together, these factors are thought to dynamically regulate neural responses in an activity-dependent manner.[25]

An example of short-term synaptic depression is found at the auditory nerve–cochlear NM (AN–NM) endbulb of Held synapse in birds.[14] This synapse is analogous to synapses onto bushy cells in the mammalian anteroventral cochlear nucleus. High rates of auditory nerve (AN) activity result in NM neurons to "lock" to a specific phase of the AN input signal, firing synchronized, and filtered initial APs.[26] Activity-dependent depression at this homogeneous but specialized synapse can be viewed as a low-pass temporal filter of presynaptic spike trains that contribute to the adaptation of postsynaptic responses at high rates of sustained sensory input. Interestingly, this form of synaptic depression occurs at early-developing NM synapses as well, but regulating factors remain largely unexplored. In this study, we revisited factors regulating short-term synaptic depression at two functionally distinct developmental time periods in the avian NM. We found that there is a developmental shift in the relative reliance on pre-, post-, and extrasynaptic factors in regulating short-term synaptic plasticity in NM.

Methods

Slice preparation. All animal procedures were performed in accordance with federal guidelines on animal welfare and approved by Northwestern University Institutional Animal Care and Use Committee. Acute brainstem slices were prepared as previously published[27–29] from White Leghorn chicken (*Gallus gallus domesticus*) embryos at two functionally distinct developmental time periods: embryonic days (E) 14–16 and E19–20. Brainstems were dissected and isolated in ice-cold oxygenated low-Ca^{2+} high-Mg^{2+}-modified artificial cerebral spinal fluid (ACSF) containing (in mM): 130 NaCl, 3 KCl, 1.25 NaH_2PO_4, 26 $NaHCO_3$, 3 $MgCl_2$, 1 $CaCl_2$, and 10 glucose. ACSF was continuously bubbled with a mixture of 95% O_2/5% CO_2 (pH 7.4, osmolarity 295–310 mOsmL). The brainstem was blocked coronally, affixed to the stage of a vibratome slicing chamber (Technical Products International), and submerged in ice-cold ACSF. Bilaterally symmetrical coronal slices were made (200–300 µm thick) and ~4–6 slices containing NM were taken along the caudal to rostral plane, representing the low- to high-frequency regions of NM, respectively. All neurons reported here were obtained from the most rostral slice of the nucleus, representing the high-frequency region of NM, a homogeneous group of neurons with similar structure and function.

Slices were collected in a custom holding chamber and allowed to equilibrate for one hour at 32°C in normal ACSF containing (in mM): 130 NaCl, 3 KCl, 1.25 NaH_2PO_4, 26 $NaHCO_3$, 1 $MgCl_2$, 3 $CaCl_2$, and 10 glucose. For experiments where external Ca^{2+} was altered (0.5, 1.0, 2.0, 3.0), the external concentration of Mg^{2+} was adjusted accordingly in order to maintain correct cationic molarity levels. The external Ca^{2+} concentration for all control data was 3 mM unless otherwise indicated. ACSF was continuously bubbled with a mixture of 95% O_2/5% CO_2 (pH 7.4, osmolarity 295–310 mOsm/L). Slices were transferred from the holding chamber to a 0.5 mL recording chamber mounted on an Olympus BX51W1 microscope for electrophysiological experiments. The microscope was equipped with a CCD camera, 60× water immersion objective, and infrared differential interference contrast optics. The recording chamber was superfused continuously by a WPX1 peristaltic pump (Welco) at near physiologic temperatures (monitored at ~33°–35°C, Warner Instruments) in oxygenated normal ACSF at a rate of 1.5–2 mL/min.

Whole-cell electrophysiology. Voltage-clamp experiments were performed using an Axon Multiclamp 700B amplifier (Molecular Devices). Patch pipettes were pulled to a tip diameter of 1–2 µm using a P-91 flaming/brown micropipette puller (Sutter) and had resistances ranging from 3 to 6 MΩ. The internal solution was cesium based containing the following (in mM): 108 $CsMeSO_3$, 5 CsCl, 1 $MgCl_2$, 15 phosphocreatine-$Tris_2$, 8 BAPTA-Cs_4, 10 HEPES, 3 QX-314.Cl, 4 MgATP, 0.4 $Tris_2$GTP, pH adjusted to 7.3 with TrisOH. The liquid junction potential was 5 mV, and data were adjusted accordingly. The Cs-based internal solution was used to block K^+ conductances, and QX-314.Cl was used to block Na^+ conductances to avoid space-clamp issues. Series resistance was compensated for by ~80% in all voltage-clamp recordings.

A small hyperpolarizing (–1 mV, 30 ms) voltage command was presented at the beginning of each recorded trace to document and monitor whole-cell parameters (resting membrane potential [RMP], cell membrane capacitance, series resistance, and input resistance). RMPs were measured immediately after break-in to avoid cesium-induced depolarization during voltage-clamp experiments. Neurons were included in the data analysis only if they had RMPs between –50 and –70 mV and had series resistances <12 MΩ. Raw data were low-pass filtered at 2 kHz and digitized at 20 kHz using a Digidata 1440A (Molecular Devices).

Pipettes were visually guided to NM, and neurons were identified and distinguished from surrounding tissue based on cell morphology and location of the nucleus within the slice. All the experiments were conducted in the presence of a $GABA_A$-R antagonist picrotoxin (PTX, 100 µM). After a GΩ seal was attained, membrane patches were ruptured, and NM neurons were held in whole-cell configuration at –60 mV (V_{CLAMP}). Isolated AMPA-R-mediated excitatory postsynaptic currents (EPSCs) were recorded in the presence of an N-methyl-D-aspartate-type glutamate receptor (NMDA-R) antagonist DL-2-amino-5-phosphonopentanoic acid (DL-APV, 100 µM). A total of 10–20 traces were obtained at a rate of 0.01 Hz for

each isolated AMPA-R-mediated EPSC. Averaged EPSCs are represented in the figures unless otherwise indicated. Desensitization of isolated AMPA-R-mediated EPSCs was blocked by bath application of cyclothiazide (CTZ, 100 μM) in some experiments (noted in results). The clearance of neurotransmitter was altered by the neural and glial glutamate transporter blocker DL-threo-β-benzyloxyaspartic acid (DL-TBOA, 100 μM), and its effect was measured from isolated AMPA-R-mediated EPSCs.

Extracellular synaptic stimulation was accomplished using a concentric bipolar electrode (tip core diameter = 125 μm, World Precision Instruments). Square electric pulses, 100 μs in duration, were delivered by an Iso-flux stimulator and a MASTER 9 current generator (A.M.P.I). Stimulating electrodes were placed in the AN root (Fig. 1A). Input–output curves were derived for each NM neuron, and the stimulus intensity was adjusted in an attempt to recruit all excitatory inputs and evoke the maximum EPSC, resulting in a plateau EPSC response. This stimulus intensity (mean = 174 ± 3.2 μA) never exceeded the output of the stimulus generator and was ~10%–20% less than the maximum intensity tolerated in this slice preparation without causing hydrolysis or motion of the stimulating electrode tip.[29] An example is shown in Figure 1B. For this individual NM neuron, the stimulus intensity was increased in 10 μA steps (up to the maximum of the stimulus isolator), and unitary AMPA-R-mediated EPSCs were recorded (plotted as the average of eight trails for each stimulus intensity). The upward gray triangle indicates stimulus intensity level used for the trace shown in Figure 1Ci.

Depending on the experimental paradigm (see results section), short-interval paired pulses or stimulus trains were used. Paired-pulse stimulus intervals (PPSI) ranged from 0.005 to 10 seconds. Stimulus trains were 10 pulses at a rate of 100 Hz delivered every 10 seconds. Figure 1Ci shows an example of an AMPA-R-mediated EPSC recorded from an E20 NM neuron using the stimulus train at ~20% below maximum strength. The AMPA-R-mediated EPSCs significantly depolarized the NM neuron only for the first two pulses in the stimulus train. As a result, the output of the NM neuron generated only two APs (Fig. 1Cii). This type of postsynaptic depression contributes to the low-pass filtering of postsynaptic AP generation during high rates of sustained AN activity. Figure 1D shows the input–output relationship of the probability of AP generation as a function of EPSC strength. Maximum EPSC strength always occurs for the first pulse, and the probability of an AP occurring is greatest. Subsequent train pulses produce EPSCs at a reduced ratio of the maximum and the probability of AP generation decreases as a function of reduced paired-pulse ratios ([PPRs] = P_N/P_1, see data analysis section). It should be noted, however, that the relative strength of subsequent EPSCs is dependent on the stimulus pulse number (eg, $P_2/P_1 = 0.25$ vs $P_{10}/P_1 = 0.01$, Fig. 1Ci). Figure 1E shows the average probability of AP generation as a function of stimulus train pulse number. Take together, synaptic depression recorded at the AN–NM synapse results in temporal filtering of AP output and is thought to be essential for encoding temporal cues used for auditory processing.

Data analysis. Recording protocols were written and run using Clampex acquisition and Clampfit analysis software (version 10.3; Molecular Devices). Statistical analyses and graphing protocols were performed using Prism (GraphPad versions 5.0a). PPR was defined as $Pulse_N/Pulse_1$, where a ratio of 1.0 represented equal amplitudes between $EPSC_N$ and $EPSC_1$. All graphic representations of data illustrate mean ±1 standard error (SE).

Reagents. Bath application of CTZ and DL-TBOA was allowed to perfuse through the recording chamber for at least 2 minutes before subsequent recordings were obtained. CTZ, DL-TBOA, DL-APV, PTX, and all other salts and chemicals were obtained from Sigma-Aldrich. QX-314 was obtained from Alomone Labs.

Results

At many neural synapses, repeated stimuli delivered at short-time intervals lead to a transient decrease in synaptic strength, that is, short-term synaptic depression. Using either short-interval paired pulses or trains of 10 pulses delivered at a rate of 100 Hz, we found that (1) late-developing (E19–20) NM neurons remain in a synaptically depressed state for at least 4 seconds following fixed intervals of paired-pulse stimulation, (2) the degree of short-term synaptic strength was largely due to exogenous calcium concentration levels and partly dependent on postsynaptic AMPA-R desensitization, and (3) neurotransmitter accumulation alters short-term synaptic depression at early-developing (E14–16) synapses, but this extrasynaptic influence has a minimal contribution at late-developing NM synapses.

Time course of recovery from different intervals of paired-pulse stimulation at late-developing NM synapses. Figure 2 shows the time range of depression in isolated AMPA-R-mediated EPSCs elicited by varying PPSI (0.005–10 seconds). Figure 2Ai shows an example trace when paired-pulse stimuli were administered at a 0.02 seconds interstimulus interval. The second EPSC amplitude was depressed by ~40% when compared to the first EPSC, resulting in a PPR of 0.62. The neuron did not recover from synaptic depression until the PPSI was six seconds (PPR = 1.04, Fig. 2Aii). This PPR was consistent for PPSIs up to 0.2 seconds across the population of E19–20 NM neurons tested (Fig. 2B, $n = 13$). Shorter PPSIs resulted in an average PPR of 0.41 ± 0.1 and 0.49 ± 0.08 for 0.005 and 0.01 seconds, respectively, while the longest PPSI (10 seconds) resulted in an average PPR of 1.1 ± 0.1. Complete recovery from synaptic depression occurred when PPSIs were greater than four seconds (Fig. 2Aii and B).

External calcium concentrations alter the strength of short-term synaptic plasticity. To investigate the contribution of presynaptic calcium influx on short-term synaptic plasticity at late-developing NM synapses, external

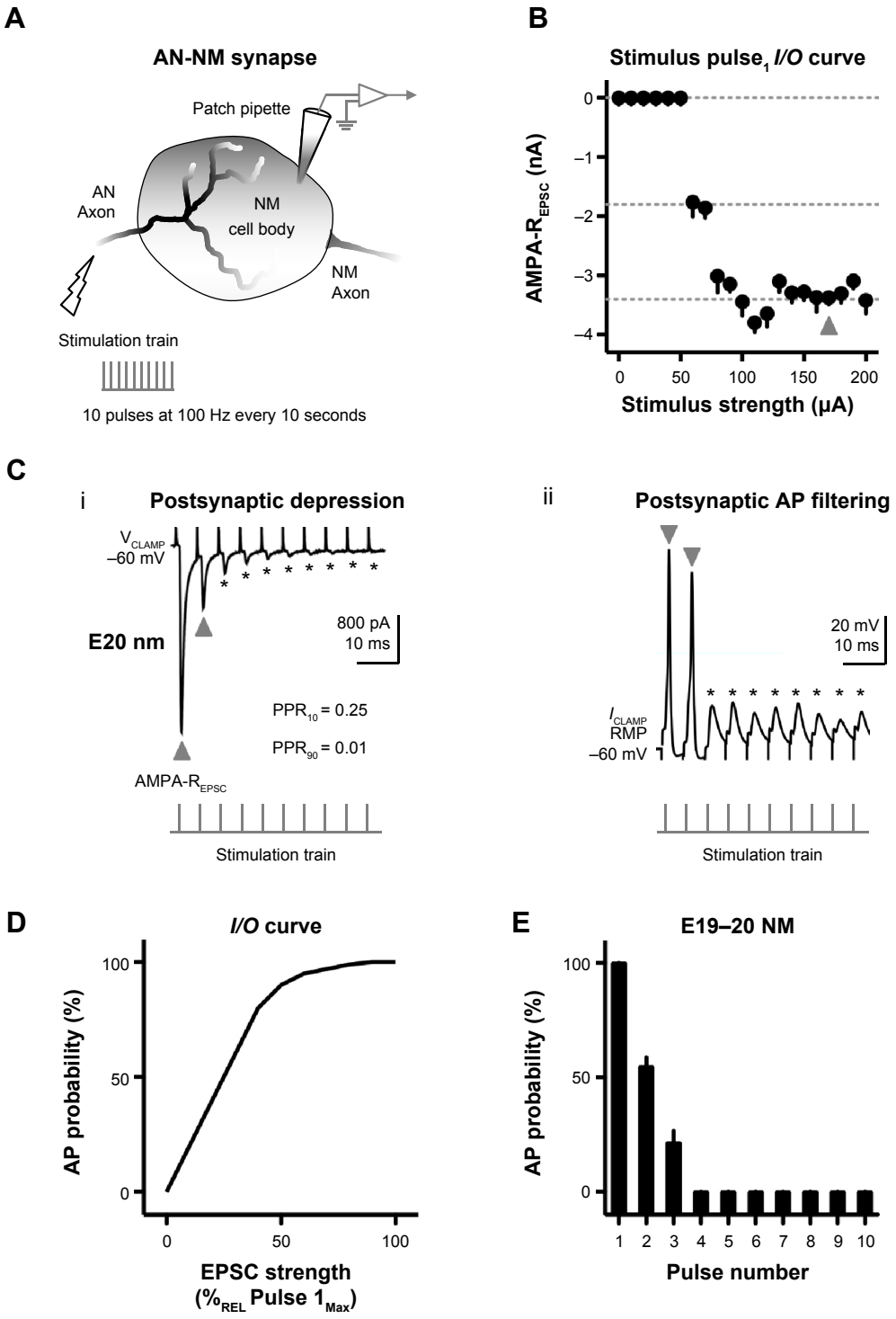

Figure 1. Synaptic depression at late developing NM synapses acts as a low-pass temporal filter. (**A**) Schematic representation of the AN–NM endbulb of Held synapse. Rate of AN stimulation = train of 10 pulses at a rate of 100 Hz, repeated every 10 seconds (lighting bolt, vertical lines, lower left). Patch pipette diagram shows experimental paradigm of voltage and current clamp traces depicted in (**C**i and **C**ii), respectively. (**B**) Input–output curve plotted for an isolated AMPA-R-mediated EPSCs as a function of stimulus intensity strength recorded from an E20 NM neuron. The *I/O* curve was derived from the EPSC response to pulse 1 of the stimulus train. Each circle represents the average of eight trials for each stimulus intensity. Upward gray triangle indicates stimulus intensity level used for the trace shown in (**C**i). Gray dashed lines indicate steps from baseline in the EPSC amplitude. (**C**i) Representative voltage clamp (V_{CLAMP}) trace of isolated AMPA-R-mediated EPSCs shows synaptic depression (same neuron in **B**). In this and subsequent figures, V_{CLAMP} –60 mV = membrane voltage at which neurons were held and recorded from. (**C**ii) Representative current clamp trace (I_{CLAMP}) recorded from the cell body of an individual NM neuron shows back propagating action potential (AP) filtering. Upward gray triangles in (Ci) represent EPSCs able to trigger APs in (**C**ii) (downward black triangles). Asterisks in (**C**i) represent reduced current responses (ie, synaptic depression) that result in the subthreshold postsynaptic potentials shown in (**C**ii, *). RMP = resting membrane potential. (**D**) Input–output curve of the average probability of AP generation as a function of EPSC strength. (**E**) Population data ($n = 7$) showing the probability of AP generation as a function of stimulus train pulse number.

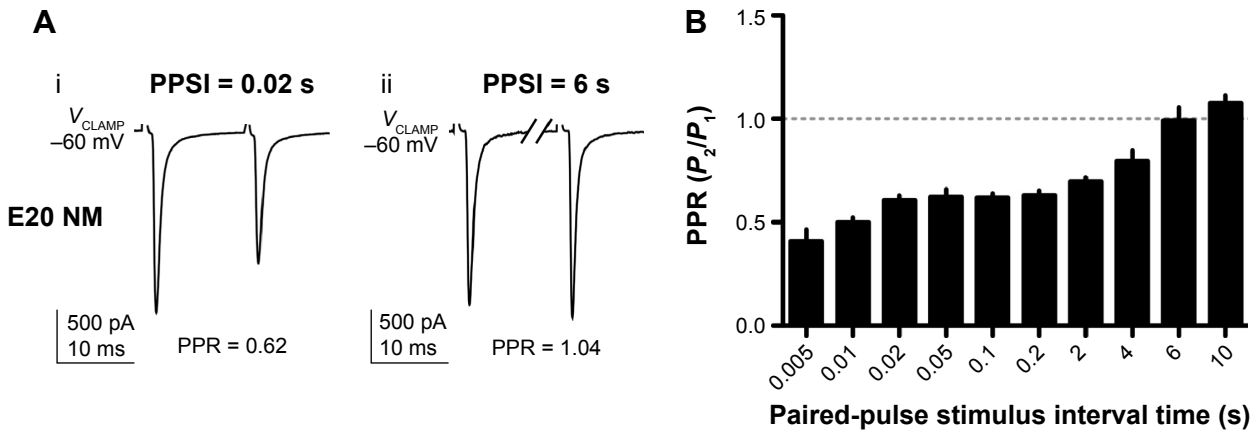

Figure 2. Time course of recovery from short-term synaptic depression at late-developing NM synapses. (**A**) Representative paired-pulse V_{CLAMP} traces of isolated AMPA-R-mediated EPSCs from the same E20 NM neuron. Paired-pulse stimulus intervals (PPSI) were systematically delivered from 0.005 to 10 seconds. For this neuron, EPSC recorded at PPSIs of 0.02 and 6 seconds are shown (**A**i and **A**ii, respectively). In this and subsequent figures, paired-pulse ratio (PPR) = unitary EPSC amplitude of the second pulse divided by the unitary EPSC amplitude of the first pulse (P_2/P_1). As PPR approaches 1, the EPSC amplitudes from both pulses are equal in magnitude and the neuron has recovered from depression. PPR values are given below each trace. Hash mark in (ii) = break in time. (**B**) Population data (n = 13) showing PPR as a function of increasing PPSIs, dashed gray line = 1:1 ratio.

calcium concentrations $[Ca^{2+}]_E$ were systematically varied from 0.5 to 3.0 mM, with paired-pulse stimuli held constant at a 50 ms time interval. Figure 3A (top row) shows representative recordings of isolated AMPA-R-mediated EPSCs during 0.5 and 1.0 mM bath-applied external calcium concentration levels. For both $[Ca^{2+}]_E$ concentration levels, the EPSC amplitude following either paired-pulse stimuli was significantly reduced when compared to 3.0 mM $[Ca^{2+}]_E$ ($P < 0.003$, Kruskal–Wallis = 14.04, Dunn's multiple post hoc comparison). For the 0.5 mM $[Ca^{2+}]_E$ level, the second EPSC was 34% larger that the first EPSC (PPR = 1.34, Fig. 3Ai), showing synaptic facilitation rather than depression. Synaptic facilitation is defined as an enhanced neural response following a pair of stimuli in which the second EPSC amplitude is greater than the first. For 1.0 mM $[Ca^{2+}]_E$, the EPSCs were nearly equal, with a PPR of 0.97 (Fig. 3Aii). Increasing external

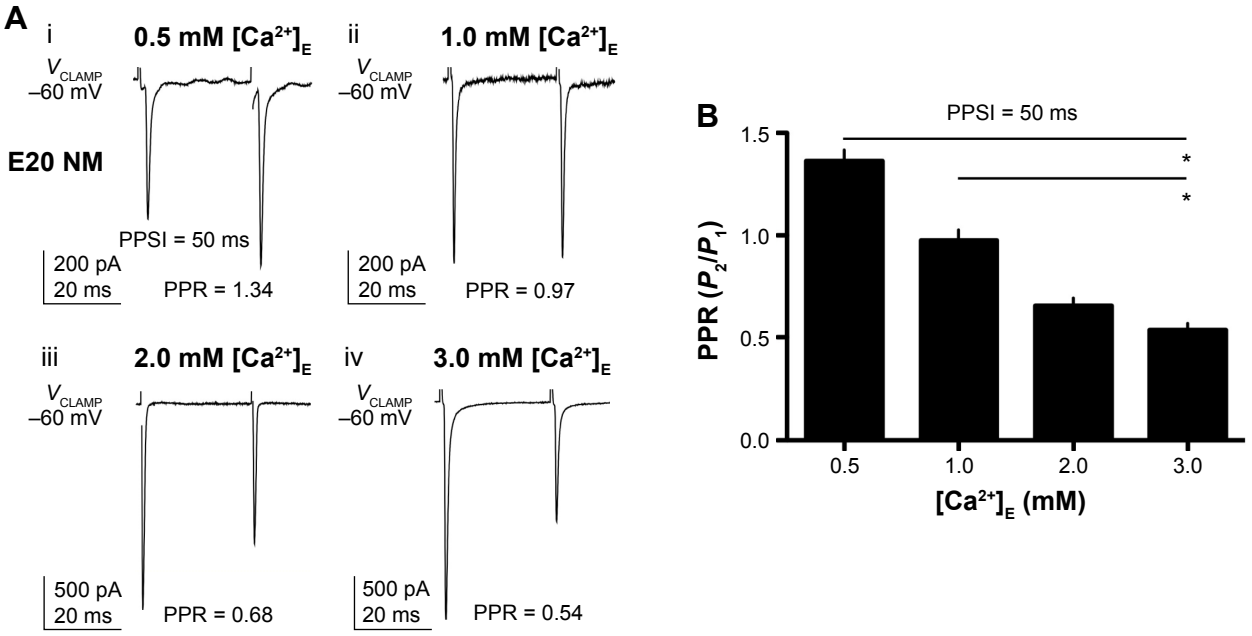

Figure 3. External $[Ca^{2+}]$ levels regulate short-term synaptic depression at late-developing NM synapses. (**A**) Representative paired-pulse V_{CLAMP} traces of isolated AMPA-R-mediated EPSCs at (i) 0.5 mM, (ii) 1.0 mM, (iii) 2.0 mM, and (iv) 3.0 mM external calcium concentration levels $[Ca^{2+}]_E$. Fixed paired-pulse stimulus interval (PPSI) = 50 ms. (**B**) Population data (n = 21) showing PPR as a function of different external Ca^{2+} concentration levels. External magnesium concentrations were adjusted accordingly to maintain equal divalent cation concentrations for each Ca^{2+} condition. In this and subsequent figures, line and asterisk present significance at $P < 0.05$.

calcium concentration levels to 2 mM changed the PPR to 0.68 (Fig. 3Aiii). At 3.0 mM $[Ca^{2+}]_E$, the recorded EPSCs following paired-pulse stimulation showed robust short-term synaptic depression, with a PPR of 0.54 (Fig. 3Aiv). These results were consistent across the population of neurons tested (Fig. 3B, $n = 21$).

Blocking postsynaptic AMPA-R desensitization alters the degree of synaptic depression at late-developing NM synapses. To address if postsynaptic factors also contribute to short-term synaptic depression at E19–20 NM synapses, we blocked the desensitization abilities of AMPA-R by bath application of 100 µM of CTZ. The degree of synaptic depression in NM neurons changed markedly during bath application of CTZ with a constant 50 ms PPSI ($Control_{PPR} = 0.51 \pm 0.10$; $CTZ_{PPR} = 0.79 \pm 0.13$, $P = 0.13$, Mann–Whitney test, data not shown), as previously reported.[14] Figure 4 shows representative traces of isolated AMPA-R-mediated EPSCs using a higher rate of stimulation, with a train of 10 pulses delivered at 100 Hz under control (Fig. 4i) and CTZ (Fig. 4ii) conditions for the same NM neuron. At this rate of AN stimulation, strong short-term synaptic depression occurred in the control condition; the PPR measured at 10 ms ($PPR_{10} = P_2/P_1$,) and 90 ms ($PPR_{90} = P_{10}/P_1$) was 0.36 and 0.07, respectively. In contrast, the PPR during bath application of CTZ changed to 0.56 and 0.25 when measured at 10 and 90 ms, respectively. Although synaptic depression occurred during CTZ, the larger PPR indicates that the degree of depression is less drastic when AMPA-R desensitization is blocked. This result was consistent across all neurons tested ($n = 9$) and across stimulation pulse numbers (Fig. 4B). Although CTZ altered the degree of synaptic depression, the amplitude of the first EPSC was unaffected (Fig. 4C), indicating that the effect of AMPA-R

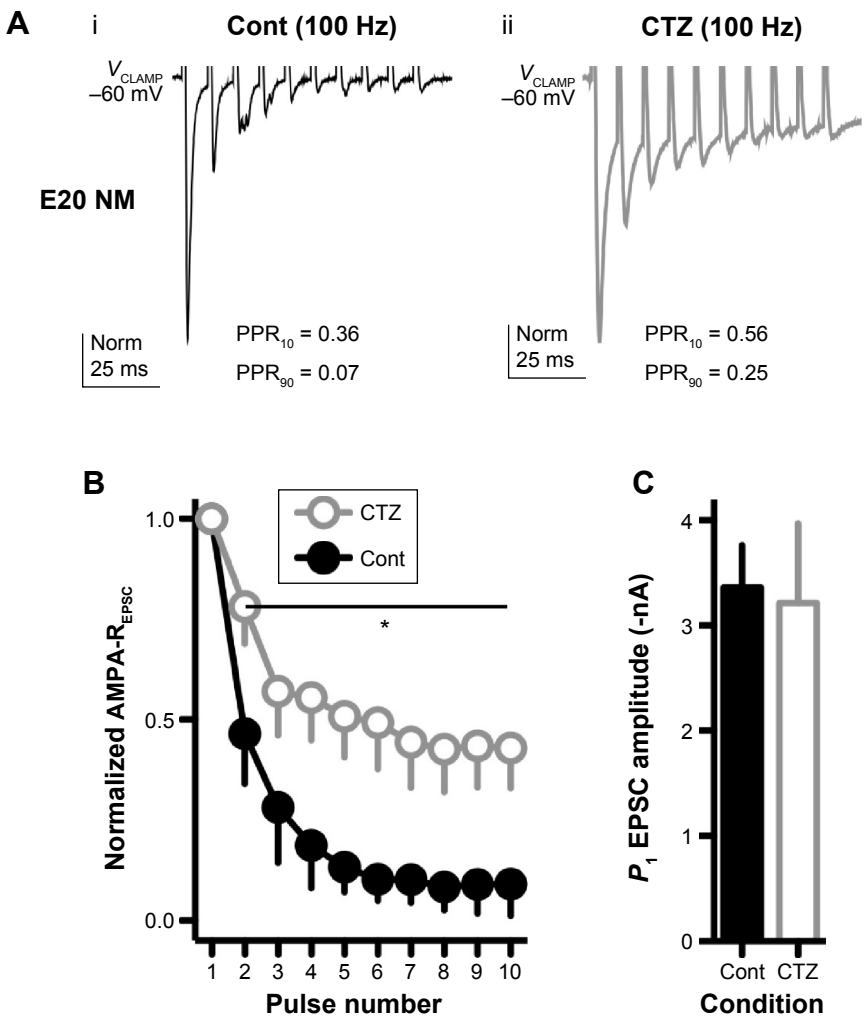

Figure 4. Short-term synaptic depression is partly dependent on AMPA-R desensitization at late-developing NM synapses. (**A**) Representative V_{CLAMP} traces of isolated AMPA-R-mediated EPSCs recorded from the same E20 NM neuron before (i, control, black trace) and during bath application of CTZ (ii, gray trace). Stimulation = 10 pulses delivered at 100 Hz repeated every 10 seconds. PPR_{10} and PPR_{90} represent PPSIs corresponding to 10 ms (P_2/P_1) and 90 ms (P_{10}/P_1) of the stimulus train, respectively. (**B**) Population data ($n = 9$) showing normalized AMPA-R-mediated EPSCs as a function of corresponding pulse number. Cont = control, CTZ = drug condition. (**C**) Population data of pulse 1 (P_1) AMPA-R-mediated EPSC amplitude as a function of experimental condition. Average drug application time for CTZ traces = 14 ± 4 minutes.

desensitization is strongest for subsequent pulses in a train of stimuli. The partial recovery from depression suggests that receptor desensitization accounts for only a portion of short-term synaptic depression observed in NM.

Short-term synaptic depression by glutamate clearance at late-developing NM synapses. We tested whether glutamate clearance contributes to short-term synaptic depression by blocking uptake with DL-TBOA, a glutamate transport blocker. First, we tested the effect of glutamate clearance on isolated AMPA-R-mediated EPSCs using low-frequency afferent stimulation. Figure 5A shows representative traces of isolated AMPA-R-mediated EPSCs recorded during control (black trace) and bath application of DL-TBOA (superimposed red trace) from the same NM neuron. Blocking glutamate clearance did not alter isolated AMPA-R-mediated EPSCs following low-frequency afferent stimulation (0.01 Hz) as previously reported.[30] Across the population of NM neurons tested (n = 10), the unitary amplitude (Fig. 5B), kinetics (Fig. 5C), nor the PPR_{50} (Fig. 5D) changed during bath application of DL-TBOA. Please note that unitary amplitude value = peak EPSC during TBOA/peak ESPC during control ($Peak_{TBOA}$/$Peak_{Cont}$). Value of 1 = no change in peak EPSC amplitude.

We next tested whether a higher rate of afferent stimulation, along with blockade of glutamate clearance, would cause a change in short-term synaptic depression in E19–20 NM neurons. Figure 6 shows representative traces of isolated

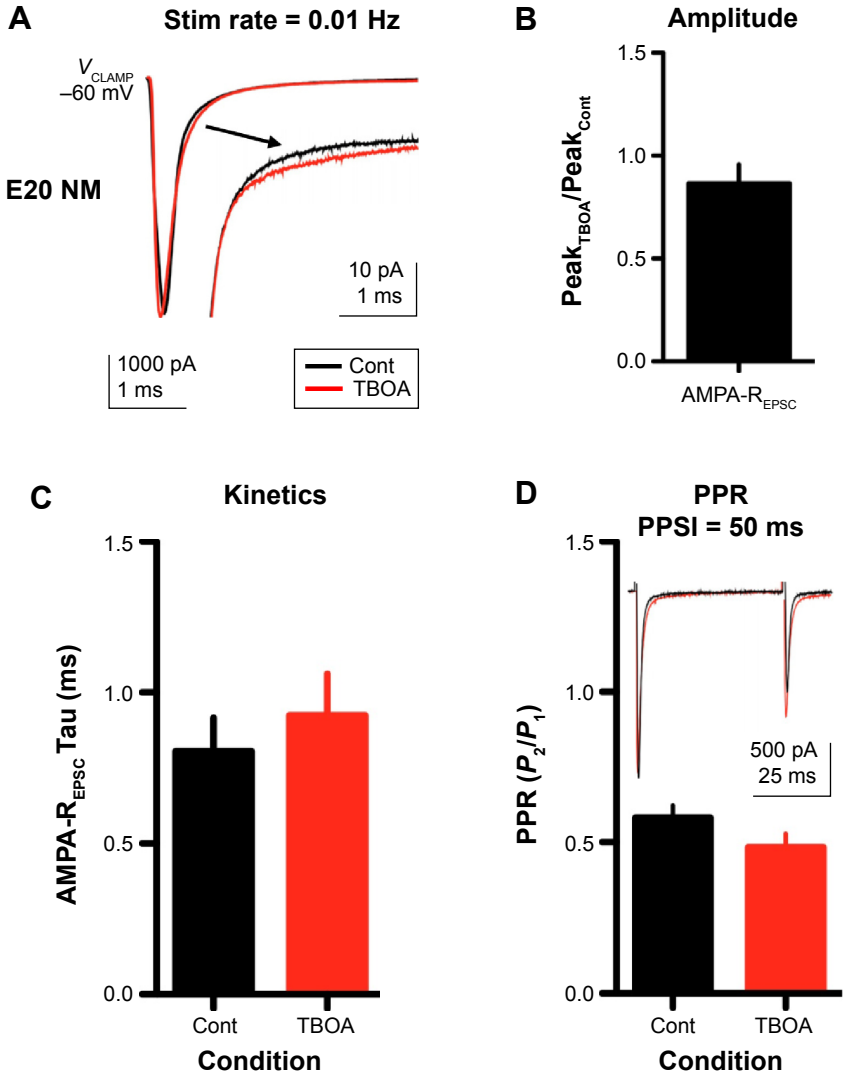

Figure 5. Bath application of TBOA, a neural and glial glutamate transport blocker, does not alter AMPA-R-mediated EPSCs properties during low-frequency stimulation at late-developing NM synapses. (**A**) Representative V_{CLAMP} traces of isolated AMPA-R-mediated EPSCs recorded from the same E20 NM neuron before (control, black trace) and during bath application of DL-threo-β-benzyloxyaspartic acid (TBOA, 100 μM, superimposed red trace). Stimulation rate = 0.01 Hz. Inset shows expanded EPSC response kinetics before and during TBOA application. (**B**) Population data (n = 10) showing the ratio change in unitary EPSC amplitude during TBOA application. Unitary amplitude value = peak EPSC during TBOA/peak ESPC during control ($Peak_{TBOA}$/$Peak_{Cont}$). Value of 1 = no change in peak EPSC amplitude. (**C**) Population data showing EPSC decay tau fit with a single exponential and (**D**) PPRs during control and TBOA conditions. Inset in (**D**) shows representative EPSCs during control (black trace) and TBOA (superimposed red trace) conditions. Cont = control, TBOA = drug condition. In this and Figure 6, average drug application time for TBOA traces = 24 ± 6 minutes.

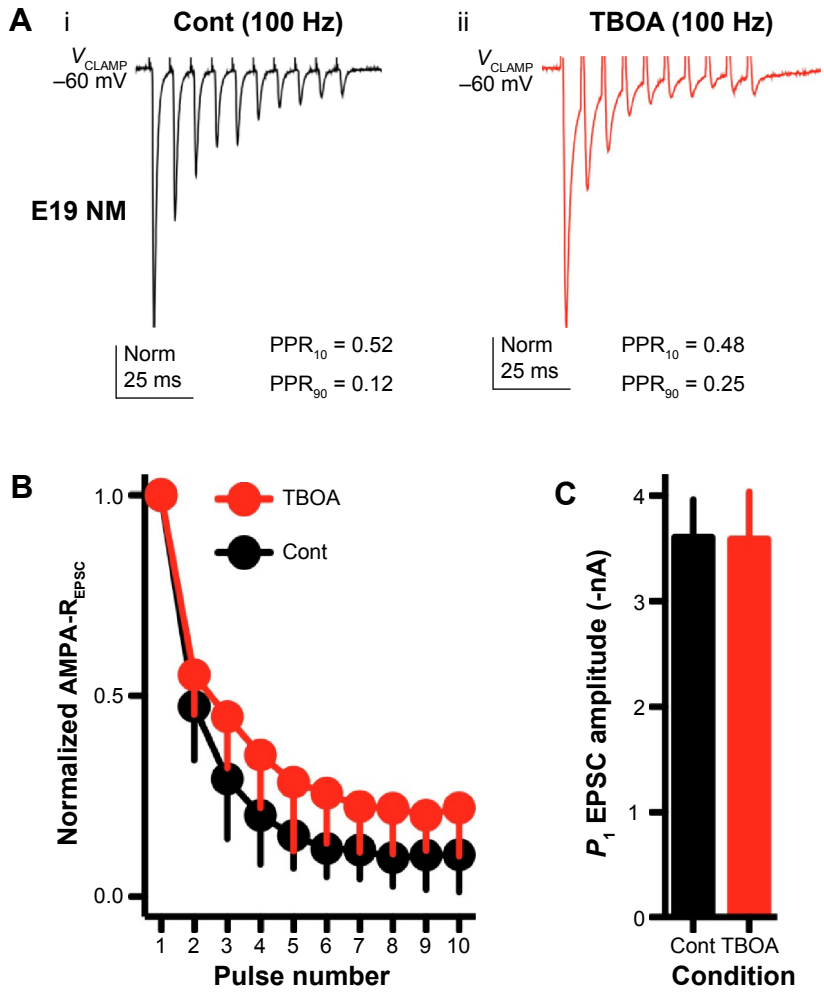

Figure 6. Short-term synaptic depression is not regulated by glutamate clearance at late-developing NM synapses. (**A**) Representative V_{CLAMP} traces of isolated AMPA-R-mediated EPSCs recorded from the same E19 NM neuron before (i, control, black trace) and during bath application of TBOA (ii, red trace). Stimulation = 10 pulses delivered at 100 Hz repeated every 10 seconds. PPR_{10} and PPR_{90} represent PPSIs corresponding to 10 ms (P_2/P_1) and 90 ms (P_{10}/P_1) of the stimulus train, respectively. (**B**) Population data (n = 10, same neurons in Fig. 5) showing normalized AMPA-R-mediated EPSCs as a function of corresponding pulse number. (**C**) Population data of pulse 1 (P_1) AMPA-R-mediated EPSC amplitude as a function of experimental condition. Cont = control, TBOA = drug condition.

AMPA-R-mediated EPSCs when a train of 10 pulses at a rate of 100 Hz was delivered under control (Fig. 6i) and DL-TBOA (Fig. 6ii) conditions for the same NM neuron. At this rate of AN stimulation, strong short-term synaptic depression occurred in the control condition; the PPR measured at 10 ms (PPR_{10} = P_2/P_1,) and 90 ms (PPR_{90} = P_{10}/P_1) was 0.52 and 0.12, respectively. The PPR during bath application of DL-TBOA remained relatively unchanged for the first pulse in the train (PPR_{10} = 0.48) but slightly changed to a PPR of 0.25 when measured at 90 ms (albeit not significant). This result was consistent across the sample of neurons tested (n = 10, same neurons from Fig. 5) as well as across stimulation pulse number (Fig. 6B and C).

Glutamate transporters shape isolated AMPA-R-mediated properties and contribute to short-term synaptic depression at early-developing NM synapses. We previously reported that the clearance of glutamate is developmentally regulated and has differential effects on AMPA-R and NMDA-R responses at early-developing synapses,[28] similar to other developing sensory synapses.[31] We therefore tested the effects of glutamate clearance in shaping isolated AMPA-R-mediated EPSCs at early-developing (E14–16) NM synapses. Blocking glutamate clearance of an E15 NM neuron significantly altered AMPA-R responses following low-frequency afferent stimulation (0.01 Hz) (Fig. 7). Representative traces of isolated AMPA-R-mediated EPSCs recorded during control (black traces) and bath application of DL-TBOA (superimposed red traces) from the same NM neuron are shown in Figure 7A. The left panel shows unitary EPSC amplitude and the right panel shows normalized responses to highlight changes in ESPC kinetics for the same neuron during both conditions. Unitary amplitude value = peak EPSC during TBOA/peak ESPC during control ($Peak_{TBOA}/Peak_{Cont}$). Value of 1 = no change in peak EPSC amplitude. Across the

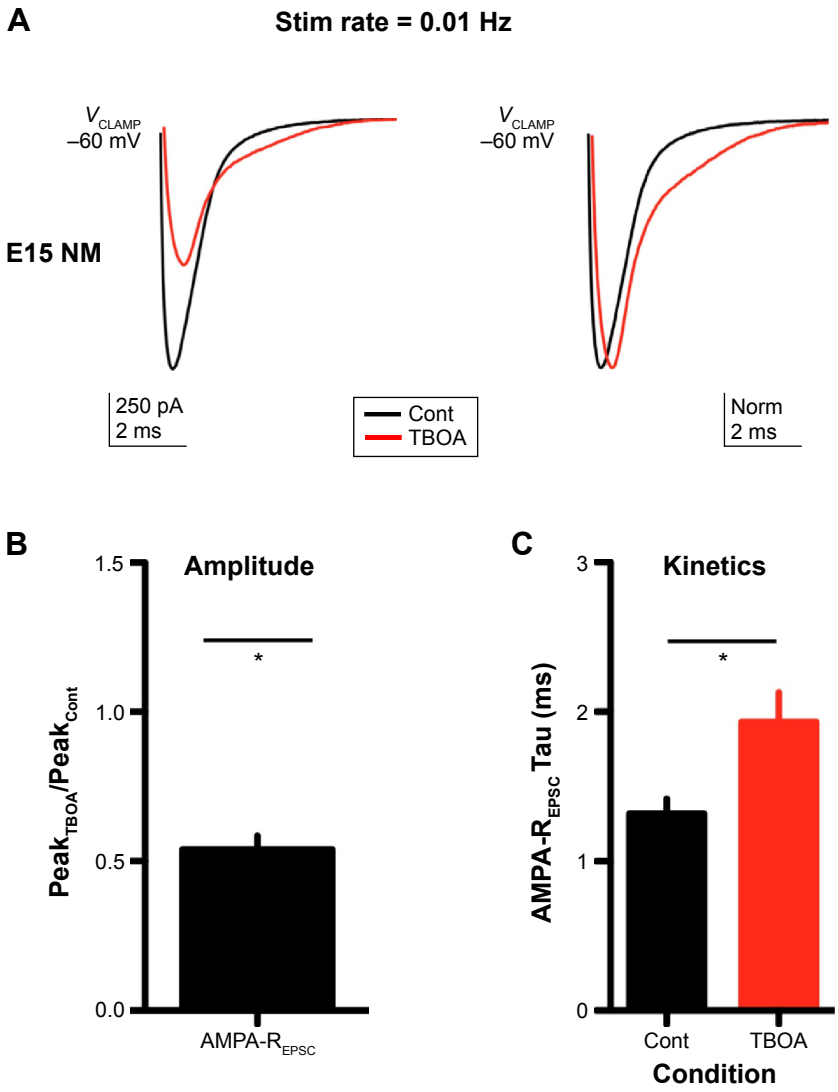

Figure 7. Glutamate transporters shape isolated AMPA-R-mediated properties during low-frequency stimulations at early-developing NM synapses. (**A**) Representative V_{CLAMP} traces of isolated AMPA-R-mediated EPSCs recorded from the same E15 NM neuron before (control, black traces) and during bath application of TBOA (100 μM, superimposed red traces). Right panel in (**A**) shows normalized traces taken from the left panel to highlight differences in EPSC response kinetics. (**B**) Population data ($n = 7$) showing the ratio change in unitary EPSC amplitude during TBOA application. Unitary amplitude value = peak EPSC during TBOA/peak ESPC in control ($Peak_{TBOA}/Peak_{Cont}$). Value of 1 = no change in peak EPSC amplitude. (**C**) Population data showing EPSC decay tau fit with single (Cont = control condition) and weighted (TBOA condition) exponentials. Average drug application time for TBOA traces = 21 ± 3 minutes.

population of NM neurons tested ($n = 12$), EPSC amplitudes were significantly smaller (Fig. 7B; $P < 0.05$, paired $t = 2.21$, degrees of freedom [df] = 11) and EPSC kinetics were significantly slower (Fig. 7C; $P < 0.01$, paired $t = 2.98$, df = 11) during DL-TBOA bath application.

We next tested whether short-term synaptic plasticity would be affected by glutamate blockade in E14–16 NM neurons. We found that for most early-developing NM neurons, a time-dependent accumulation of neurotransmitter following glutamate transporter blockade changes short-term synaptic dynamics from depression to facilitation. Figure 8A shows representative traces of an isolated AMPA-R-mediated ESPCs using a fixed 50 ms PPSI. During the control condition, the PPR was 0.59 (Fig. 8Ai) and was not different compared to late-developing NM neurons during the 3 mM $[Ca^{2+}]_E$ condition (see Fig. 3Aiv and B far right column), suggesting the probability of neurotransmitter release is high at both age groups, consistent with our previously published report.[29] For the same NM neuron, bath application of DL-TBOA had a time-dependent effect on synaptic dynamics. After 12 and 22 minutes of administration of DL-TBOA, short-term synaptic depression changed to facilitation, resulting in PPRs of 0.95 and 1.21, respectively (Fig. 8Aii and Aiii). Individual traces are shown to highlight trial-to-trial variation in EPSCs during drug conditions. Across the population of NM neurons tested ($n = 8$), isolated AMPA-R-mediated EPSC kinetics significantly changed during the DL-TBOA application for both pulses 1 and 2 of the paired-pulse stimuli

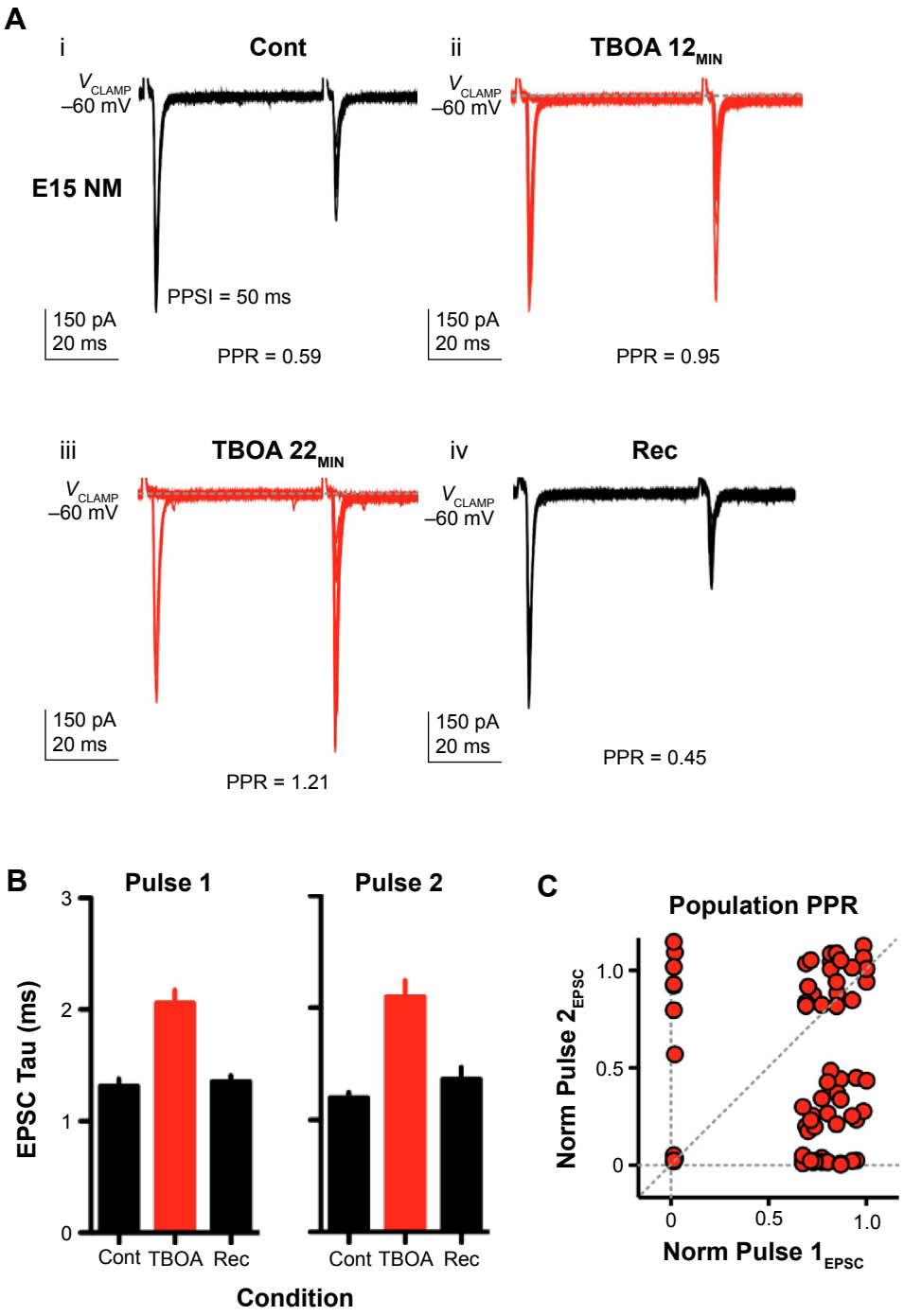

Figure 8. Accumulation of neurotransmitter following glutamate transporter blockade alters short-term synaptic depression at early-developing NM synapses. (**A**) Representative V_{CLAMP} traces of isolated AMPA-R-mediated EPSCs (10 superimposed) recorded from the same E15 NM neuron before (i, control, black traces) during bath application of TBOA (ii–iii, red traces, 100 μM) and after drug (iv, recovery, black traces). Fixed paired-pulse stimulus interval (PPSI) = 50 ms. TBOA 12_{MIN} and 22_{MIN} = selected time points of 12 and 22 minutes after TBOA application. (**B**) Population data ($n = 8$) showing EPSC decay tau fit with single (Cont = control condition) and weighted (TBOA condition) exponentials for both paired pulses. Rec = recovery condition. (**C**) Population data showing individual PPR traces ($n = 80$ traces) for each E14–16 NM neuron ($n = 8$ neurons). Unitary EPSC amplitudes were normalized (NORM) for each paired pulse (Pulse 1_{EPSC} and 2_{EPSC}) based on maximum responses. Horizontal and vertical gray dashed lines represent EPSC failures for the second or first paired pulse, respectively. Gray diagonal dashed line represents a PPR = 1.

(Fig. 8B; $P < 0.01$, paired $t = 3.78$, df = 7). Because of the trial-to-trial variation in EPSCs and the time-dependent accumulation of neurotransmitter, we normalized the maximum EPSC amplitude of each individual trace across the population of NM neurons tested (~10 traces for each NM neuron) 20 minutes after bath application of DL-TBOA. Normalized pulse 1 EPSC amplitudes were then compared to normalized pulse 2 EPSC amplitudes. When analyzed in

this way, we found that NM neurons responded differentially to DL-TBOA; nearly 25% stayed depressed, 25% resulted in a complete EPSC elimination following either the first, second, or both paired pulses, and 50% changed from short-term synaptic depression to facilitation (Fig. 8C).

Discussion

Mechanisms regulating short-term synaptic depression are well documented to include pre-, post-, and extrasynaptic factors.[4,5,25] We report here that short-term synaptic depression lasts as long as four seconds at late-developing avian AN–NM synapses and is largely dependent on presynaptic exogenous calcium levels and, to a lesser extent, on postsynaptic AMPA-R desensitization. We also report that extrasynaptic factors do not play a substantial role in regulating synaptic dynamics at late-developing synapses but significantly alter short-term synaptic dynamics at early-developing NM synapses by changing a portion of AMPA-R-mediated EPSCs from depression to facilitation.

Presynaptic mechanisms. Presynaptic APs trigger varying amounts of neurotransmitter release and can thereby influence the output firing of their postsynaptic targets. When repeated APs are separated by only tens of milliseconds, postsynaptic target neurons can show a transient decrease in synaptic strength, or short-term synaptic depression, through reduced EPSCs.[32]

A primary mechanism that regulates synaptic depression is presynaptic calcium influx.[33] The initial release probability of neurotransmitter is dependent on exogenous calcium concentration levels and its subsequent influx,[34,35] leading to varying postsynaptic EPSC strengths.[36] Other presynaptic factors include the depletion of available neurotransmitter and inactivation of calcium release sites.[12,13,37] Depletion of neurotransmitter is dependent on the number of vesicles ready to be released (ie, readily releasable pool [RRP]) and on their release probability.[7,38] Stimuli delivered before the RRP is replenished results in fewer released vesicles.[39] Even if the RRP is not completely depleted, fusion of subsequent vesicles at the release site is limited due to the inactivation at that site. Recovery from synaptic depression is thought to reflect the time it takes to clear fused vesicles from the inactive release site of the membrane and the time it takes for the RRP to be refilled, which can range from milliseconds to seconds. At low enough levels, very little calcium enters the presynaptic terminal upon AP activation and the probability of neurotransmitter release is reduced. In such a low calcium environment, the buildup of residual calcium from the first AP can have a significant effect, contributing to more neurotransmitter release after the arrival of the second AP, resulting in short-term synaptic facilitation.[40,41]

However, at numerous synapses in the brain, including some neocortical and vestibular synapses, properties of synaptic depression are not consistent with depletion of the RRP.[42,43] Variations in exogenous calcium influx are thought to account for differences between synapses.[9] We observed that synaptic depression is largely dependent on presynaptic exogenous calcium influx at AN–NM synapses. During fixed paired-pulse stimulation rates, alteration of external calcium concentration levels changed short-term synaptic plasticity from strong synaptic depression (3 mM external calcium) to facilitation (0.5 mM external calcium) in AMPA-R-mediated EPSCs. Synaptic depression and facilitation can therefore occur at the same AN–NM synapse but which one dominates appears to be regulated by exogenous calcium concentration levels.

Postsynaptic considerations. Postsynaptic factors can also regulate short-term synaptic plasticity in concert with presynaptic mechanisms. It is established at the avian AN–NM synapse—as well as the mammalian retinogeniculate, the endbulb of Held, and the calyx of Held synapses—that postsynaptic effects of synaptic depression occur by AMPA-R desensitization.[12–14,18,19,44–47]

However, desensitization is related to the AMPA-Rs' ability to close and enter a nonconducting state,[15] and the accumulation of glutamate can have differential effects on AMPA-R desensitization.[14,48] This differential desensitization to glutamate is activity dependent, synapse specific, and receptor contingent, and as such will result in varying degrees of regulation of postsynaptic strength.[5] At retinogeniculate synapses, for example, AMPA-R desensitization contributes to a reduction in AMPA-R responses during realistic patterns of activity,[47] while desensitization at bipolar and cone synapses of the retina are differentially distributed between AMPA- and kainate receptors.[49]

In NM, the structure of the endbulb synapse, the probability of neurotransmitter release, and the time course of glutamate clearance may dictate the extent to which AMPA-R desensitization plays a role in synaptic depression. For the auditory brainstem, the high level of desensitization and the differential effect on short-term plasticity are likely due to numerous factors, including its structural features: endbulb and calyceal terminals in the avian and mammalian cochlear nucleus, as well as the medial nuclei of the trapezoid body, have a clustering of release sites positioned close together.[25] Because of the many closely spaced release sites and the high probability of neurotransmitter release at calyceal synapses, glutamate emanating from one site can diffuse, activate, and desensitize neighboring receptors, and thereby increase AMPA-R desensitization.

Another consideration regarding the strength of AMPA-R desensitization includes the age of the animal studied.[2] Wang et al showed that desensitization is stronger for young animals and contributes significantly to synaptic depression, whereas older animals present with less AMPA-R desensitization and recover from depression more quickly after neurotransmitter release.[50] Desensitization in older animals is, therefore, more apparent only at high rates of afferent activation, with the sensitivity of desensitization possibly due to developmental changes in AMPA-R subunit composition.

Glutamate clearance. Although pre- and postsynaptic factors strongly influence synaptic dynamics, glutamate clearance from the synapse plays a role as well, especially during high rates of presynaptic activity.[21] We previously reported that glutamate clearance at the avian nucleus laminaris (NL), the downstream nucleus that receives excitatory inputs from NM, is inefficient and likely relies on neurotransmitter diffusion—rather than glutamate transporter uptake—at very early-developing synapses.[28] Otis et al indicated that glutamate clearance in NM has little effect on the peak and initial kinetics of AMPA-R responses in late-developing embryos, mirroring results of the present study. Instead, the role of glutamate clearance can be seen in a slow, small component of the AMPA-R-mediated EPSC.[51] This component can be significant in times of high activity, which NM neurons are often exposed to in ovo as part of the developmental process.[52,53]

Blocking glutamate clearance had a minimal role in regulating short-term synaptic properties in late-developing NM neurons at relatively low stimulation rates and the degree of change is dependent on the rate of afferent activity. We did not observe a strong effect upon TBOA application using a 100 Hz stimulus trains in late-developing NM synapses. A previous report has shown that the above stimulation rates of 20 Hz, blockade of transporters only slightly enhances depression, with the largest effects observed at high stimulation rates (>300 Hz).[30] In addition, we used older and narrower range of embryonic ages (E19–21), and all neurons sampled in the current study were taken from the high-frequency region, where only one-to-two afferent inputs make contact with an individual NM cell body. Oline and Burger[54] recently reported that short-term synaptic depression at AN–NM synapses varies systematically across the tonotopic axis. Differences in our study may be due to such variations.

It has also been reported that after synapse formation in NM, the rate of AMPA-R desensitization increases.[55] This is likely due to a change in subunit composition or subunit conformation, which is often associated with changes in AMPA-R-mediated EPSCs.[56,57] It is possible that the maturation of NM mirrors that of NL in this regard. NL undergoes a developmental switch in AMPA-R subunit content, changing from GluA2-containing to GluA2-lacking receptors, which contributes to rapid EPSC kinetics, calcium permeability, and inward rectification.[29] Regardless of the subunit change and its functional contributions, the lack of effect upon TBOA application indicates AMPA-Rs in NM are rapidly desensitizing by E19, with glutamate clearance factoring little into the amplitude and kinetics of AMPA-R responses from at least high-frequency placed neurons. Glutamate clearance may also have an impact on NMDA-R currents and on reducing spillover to neighboring synapses.[58] Further research is needed to reveal the role of glutamate transporters at late-developing endbulb of Held synapses in a frequency-specific manner.

During the earlier developmental period of E14–16, however, blocking glutamate clearance with TBOA application produced a strong effect. It has been reported that high-synaptic activity can increase the build up of glutamate concentration and activate presynaptic metabotropic glutamate receptors (mGluRs),[59] altering postsynaptic excitation via a presynaptic mechanism.[60] The presence of presynaptic mGluRs may explain the difference in patterns expressed by E14–16 versus E19–21 NM neurons upon TBOA application. Group II/III presynaptic mGluRs have been associated with increased PPRs upon transporter blockade and have been found at the calyx of Held[61] and retinogeniculate synapse,[62] both of which experience long bursts of spontaneous high frequency activity during development, similar to NM.[52] These two studies also found a developmental downregulation in mGluR-mediated responses. Similar to these studies, we also see an increase in the PPR upon TBOA application only at a particular developmental age (E14–16). Although NM is not exactly analogous to the calyx of Held or the retinogeniculate synapse, the comparable patterns we see in NM imply the presence of presynaptic mGluRs, similarly downregulated with development. mGluRs have been found to have a large effect in NM, especially through mediating calcium regulation.[63,64] However, the calcium mediation occurred through postsynaptic group 1 mGluRs and, although presynaptic mGluRs have been found in NM, their expression pattern appeared to be only on inhibitory inputs of late-developing NM synapses.[65,66] The developmental expression of mGluRs on excitatory inputs to NM is not known. Further work is required to see if the developmental expression of presynaptic mGluRs on afferent excitatory AN inputs helps to control high bursts of developmental activity and sculpt NM synaptic properties.

While presynaptic mGluRs may restrict calcium influx and reduce the probability of release at early-developing NM synapses, presynaptic $GABA_B$-Rs have already been shown to have a similar effect.[36,67–69] At the mammalian endbulb synapse, the activation of $GABA_B$-Rs by agonist application reduces probability of release, decreases EPSC amplitudes, and changes paired-pulse responses from depression to facilitation,[68] a result observed in the current study. Interestingly, although the effect of mGluRs is similar to that of $GABA_B$-Rs, they are differentiated by their method of activation. While the mGluRs would be activated in response to local high rates of activity and build up of glutamate, $GABA_B$-Rs are mostly activated through top down projections from higher order nuclei. Perhaps, the reason for this redundancy is fundamentally different purposes: $GABA_B$-Rs could help to control firing when functionally relevant, while mGluRs serve to prevent overexcitation during times of heavy activity at early-developing synapses. If mGluRs are present presynaptically, it is interesting to consider the functional reasons for the redundancy between the two systems. Further investigation is needed to elucidate these differences and the roles they play in regulating short-term synaptic plasticity.

Conclusion

Short-term synaptic plasticity is critical for appropriate processing of sensory information. In the auditory brainstem, the combination of presynaptic exogenous calcium levels, postsynaptic receptor desensitization, and glutamate clearance assists neurons in screening high rates of synaptic information, often acting as a low-pass temporal filter. Neurons that express synaptic depression preferentially encode the onset of a high-frequency stimulus. This improves temporal precision by reducing the value of poorly timed inputs relative to precisely timed inputs. As such, synaptic depression is thought responsible for encoding time elements of sound by preserving information about interaural time delays, providing cues used for sound localization and temporal processing.[3,70]

In this study, we revisited pre-, post-, and extrasynaptic factors and explored their effectiveness in regulating synaptic strength at two distinct developmental time periods. Using varied PPSI of AN activation, we found that the time course of synaptic depression in NM lasts as long as four seconds at late-developing synapses. To a large extent, this synaptic depression was dependent on an exogenous Ca^{2+}-dependent probability of presynaptic neurotransmitter release, and to a lesser extent, on desensitization of postsynaptic AMPA-Rs. Interestingly, extrasynaptic factors did not play a significant role in regulating synaptic strength at late-developing synapses as previously shown, as blocking glutamate clearance did not change short-term synaptic depression. In contrast, during a period of considerable synaptic refinement, blockade of glutamate clearance significantly altered synaptic strength, changing responses from depression to facilitation. These results suggest that late-developing synapses in the avian NM rely heavily on presynaptic mechanisms and to a lesser extent on postsynaptic factors, while early-developing synapses utilize both pre- and extrasynaptic mechanism to regulate synaptic dynamics.

Acknowledgments

The authors would like to thank members of the Central Auditory Physiology Laboratory and Dr. Mary Ann Cheatham and Dr. Jon Siegel for helpful discussions about the data, as well as Dr. Armin Seidl, Suzanne LaBelle, and Seema Ghelani for constructive comments on earlier versions of the manuscript. Work performed by KQ was in partial fulfillment of an AuD degree in audiology at Northwestern University, Evanston, IL.

Author Contributions

Conceived and designed the experiments: JTS and SOM. Analyzed the data: JTS, KQ, and SOM. Wrote the first draft of the manuscript: JTS, KQ, and SOM. Contributed to the writing of the manuscript: JTS, KQ, and SOM. Agreed with manuscript results and conclusions: JTS, KQ, and SOM. Jointly developed the structure and arguments for the paper: JTS and SOM. Made critical revisions and approved the final version: JTS, KQ, and SOM. All authors reviewed and approved the final manuscript.

REFERENCES

1. Abbott LF, Regehr WG. Synaptic computation. *Nature*. 2004;431(7010):796–803.
2. Wang Y, O'Donohue H, Manis P. Short-term plasticity and auditory processing in the ventral cochlear nucleus of normal and hearing-impaired animals. *Hear Res*. 2011;279(1–2):131–139.
3. Kuba H, Koyano K, Ohmori H. Synaptic depression improves coincidence detection in the nucleus laminaris in brainstem slices of the chick embryo. *Eur J Neurosci*. 2002;15(6):984–990.
4. Fortune ES, Rose GJ. Short-term synaptic plasticity as a temporal filter. *Trends Neurosci*. 2001;24(7):381–385.
5. Zucker RS, Regehr WG. Short-term synaptic plasticity. *Annu Rev Physiol*. 2002; 64:355–405.
6. Fioravante D, Regehr WG. Short-term forms of presynaptic plasticity. *Curr Opin Neurobiol*. 2011;21(2):269–274.
7. Rizzoli SO, Betz WJ. Synaptic vesicle pools. *Nat Rev Neurosci*. 2005;6(1):57–69.
8. Wang Y, Manis PB. Short-term synaptic depression and recovery at the mature mammalian endbulb of Held synapse in mice. *J Neurophysiol*. 2008;100(3): 1255–1264.
9. Neher E, Sakaba T. Multiple roles of calcium ions in the regulation of neurotransmitter release. *Neuron*. 2008;59(6):861–872.
10. von Gersdorff H, Borst JG. Short-term plasticity at the calyx of Held. *Nat Rev Neurosci*. 2002;3(1):53–64.
11. Catterall WA, Few AP. Calcium channel regulation and presynaptic plasticity. *Neuron*. 2008;59(6):882–901.
12. Bellingham MC, Walmsley B. A novel presynaptic inhibitory mechanism underlies paired pulse depression at a fast central synapse. *Neuron*. 1999;23(1):159–170.
13. Yang H, Xu-Friedman MA. Relative roles of different mechanisms of depression at the mouse endbulb of Held. *J Neurophysiol*. 2008;99(5):2510–2521.
14. Trussell LO, Zhang S, Raman IM. Desensitization of AMPA receptors upon multiquantal neurotransmitter release. *Neuron*. 1993;10(6):1185–1196.
15. Trussell LO, Fischbach GD. Glutamate receptor desensitization and its role in synaptic transmission. *Neuron*. 1989;3(2):209–218.
16. Raman IM, Trussell LO. The mechanism of alpha-amino-3-hydroxy-5-methyl-4-isoxazolepropionate receptor desensitization after removal of glutamate. *Biophys J*. 1995;68(1):137–146.
17. Bellingham MC, Lim R, Walmsley B. Developmental changes in EPSC quantal size and quantal content at a central glutamatergic synapse in rat. *J Physiol*. 1998; 511(pt 3):861–869.
18. Chanda S, Xu-Friedman MA. A low-affinity antagonist reveals saturation and desensitization in mature synapses in the auditory brain stem. *J Neurophysiol*. 2010;103(4):1915–1926.
19. Ishikawa T, Takahashi T. Mechanisms underlying presynaptic facilitatory effect of cyclothiazide at the calyx of Held of juvenile rats. *J Physiol*. 2001;533(pt 2): 423–431.
20. Jones MV, Westbrook GL. The impact of receptor desensitization on fast synaptic transmission. *Trends Neurosci*. 1996;19(3):96–101.
21. Tzingounis AV, Wadiche JI. Glutamate transporters: confining runaway excitation by shaping synaptic transmission. *Nat Rev Neurosci*. 2007;8(12):935–947.
22. Partin KM, Patneau DK, Mayer ML. Cyclothiazide differentially modulates desensitization of alpha-amino-3-hydroxy-5-methyl-4-isoxazolepropionic acid receptor splice variants. *Mol Pharmacol*. 1994;46(1):129–138.
23. Fucile S, Miledi R, Eusebi F. Effects of cyclothiazide on GluR1/AMPA receptors. *Proc Natl Acad Sci U S A*. 2006;103(8):2943–2947.
24. Diamond JS, Jahr CE. Asynchronous release of synaptic vesicles determines the time course of the AMPA receptor-mediated EPSC. *Neuron*. 1995;15(5):1097–1107.
25. Xu-Friedman MA, Regehr WG. Structural contributions to short-term synaptic plasticity. *Physiol Rev*. 2004;84(1):69–85.
26. Warchol ME, Dallos P. Neural coding in the chick cochlear nucleus. *J Comp Physiol A*. 1990;166(5):721–734.
27. Sanchez JT, Seidl AH, Rubel EW, Barria A. Preparation and culture of chicken auditory brainstem slices. *J Vis Exp*. 2011;(49):1–4.
28. Sanchez JT, Seidl AH, Rubel EW, Barria A. Control of neuronal excitability by NMDA-type glutamate receptors in early developing binaural auditory neurons. *J Physiol*. 2012;590(pt 19):4801–4818.
29. Sanchez JT, Wang Y, Rubel EW, Barria A. Development of glutamatergic synaptic transmission in binaural auditory neurons. *J Neurophysiol*. 2010;104(3): 1774–1789.
30. Turecek R, Trussell LO. Control of synaptic depression by glutamate transporters. *J Neurosci*. 2000;20(5):2054–2063.
31. Kidd FL, Isaac JT. Glutamate transport blockade has a differential effect on AMPA and NMDA receptor-mediated synaptic transmission in the developing barrel cortex. *Neuropharmacology*. 2000;39(5):725–732.

32. Abbott LF, Varela JA, Sen K, Nelson SB. Synaptic depression and cortical gain control. *Science*. 1997;275(5297):220–224.
33. Lundberg A, Quilisch H. On the effect of calcium on presynaptic potentiation and depression at the neuro-muscular junction. *Acta Physiol Scand Suppl*. 1953; 111:121–129.
34. Sudhof TC. The synaptic vesicle cycle: a cascade of protein-protein interactions. *Nature*. 1995;375(6533):645–653.
35. Li C, Ullrich B, Zhang JZ, Anderson RG, Brose N, Sudhof TC. Ca(2+)-dependent and -independent activities of neural and non-neural synaptotagmins. *Nature*. 1995;375(6532):594–599.
36. Brenowitz S, Trussell LO. Minimizing synaptic depression by control of release probability. *J Neurosci*. 2001;21(6):1857–1867.
37. Brenowitz S, David J, Trussell L. Enhancement of synaptic efficacy by presynaptic GABA(B) receptors. *Neuron*. 1998;20(1):135–141.
38. Denker A, Rizzoli SO. Synaptic vesicle pools: an update. *Front Synaptic Neurosci*. 2010;2:135.
39. Betz WJ. Depression of transmitter release at the neuromuscular junction of the frog. *J Physiol*. 1970;206(3):629–644.
40. Delaney KR, Tank DW. A quantitative measurement of the dependence of short-term synaptic enhancement on presynaptic residual calcium. *J Neurosci*. 1994; 14(10):5885–5902.
41. Regehr WG, Delaney KR, Tank DW. The role of presynaptic calcium in short-term enhancement at the hippocampal mossy fiber synapse. *J Neurosci*. 1994; 14(2):523–537.
42. Bagnall MW, McElvain LE, Faulstich M, du Lac S. Frequency-independent synaptic transmission supports a linear vestibular behavior. *Neuron*. 2008;60(2): 343–352.
43. Thomson AM, Bannister AP. Release-independent depression at pyramidal inputs onto specific cell targets: dual recordings in slices of rat cortex. *J Physiol*. 1999;519(pt 1):57–70.
44. Otis T, Zhang S, Trussell LO. Direct measurement of AMPA receptor desensitization induced by glutamatergic synaptic transmission. *J Neurosci*. 1996; 16(23):7496–7504.
45. Isaacson JS, Walmsley B. Amplitude and time course of spontaneous and evoked excitatory postsynaptic currents in bushy cells of the anteroventral cochlear nucleus. *J Neurophysiol*. 1996;76(3):1566–1571.
46. Oleskevich S, Clements J, Walmsley B. Release probability modulates short-term plasticity at a rat giant terminal. *J Physiol*. 2000;524(pt 2):513–523.
47. Chen C, Blitz DM, Regehr WG. Contributions of receptor desensitization and saturation to plasticity at the retinogeniculate synapse. *Neuron*. 2002;33(5): 779–788.
48. Trussell LO, Thio LL, Zorumski CF, Fischbach GD. Rapid desensitization of glutamate receptors in vertebrate central neurons. *Proc Natl Acad Sci U S A*. 1988; 85(12):4562–4566.
49. DeVries SH. Bipolar cells use kainate and AMPA receptors to filter visual information into separate channels. *Neuron*. 2000;28(3):847–856.
50. Wang Y, Ren C, Manis PB. Endbulb synaptic depression within the range of presynaptic spontaneous firing and its impact on the firing reliability of cochlear nucleus bushy neurons. *Hear Res*. 2010;270(1–2):101–109.
51. Otis TS, Wu YC, Trussell LO. Delayed clearance of transmitter and the role of glutamate transporters at synapses with multiple release sites. *J Neurosci*. 1996; 16(5):1634–1644.
52. Lippe WR. Rhythmic spontaneous activity in the developing avian auditory system. *J Neurosci*. 1994;14(3 pt 2):1486–1495.
53. Lippe WR. Relationship between frequency of spontaneous bursting and tonotopic position in the developing avian auditory system. *Brain Res*. 1995;703(1–2): 205–213.
54. Oline SN, Burger RM. Short-term synaptic depression is topographically distributed in the cochlear nucleus of the chicken. *J Neurosci*. 2014;34(4):1314–1324.
55. Lawrence JJ, Trussell LO. Long-term specification of AMPA receptor properties after synapse formation. *J Neurosci*. 2000;20(13):4864–4870.
56. Mosbacher J, Schoepfer R, Monyer H, Burnashev N, Seeburg PH, Ruppersberg JP. A molecular determinant for submillisecond desensitization in glutamate receptors. *Science*. 1994;266(5187):1059–1062.
57. Pei W, Huang Z, Wang C, Han Y, Park JS, Niu L. Flip and flop: a molecular determinant for AMPA receptor channel opening. *Biochemistry*. 2009;48(17): 3767–3777.
58. Kessler JP. Control of cleft glutamate concentration and glutamate spill-out by perisynaptic glia: uptake and diffusion barriers. *PLoS One*. 2013;8(8):e70791.
59. Scanziani M, Salin PA, Vogt KE, Malenka RC, Nicoll RA. Use-dependent increases in glutamate concentration activate presynaptic metabotropic glutamate receptors. *Nature*. 1997;385(6617):630–634.
60. Maki R, Robinson MB, Dichter MA. The glutamate uptake inhibitor L-trans-pyrrolidine-2,4-dicarboxylate depresses excitatory synaptic transmission via a presynaptic mechanism in cultured hippocampal neurons. *J Neurosci*. 1994;14(11 pt 1): 6754–6762.
61. Renden R, Taschenberger H, Puente N, et al. Glutamate transporter studies reveal the pruning of metabotropic glutamate receptors and absence of AMPA receptor desensitization at mature calyx of Held synapses. *J Neurosci*. 2005;25(37):8482–8497.
62. Hauser JL, Edson EB, Hooks BM, Chen C. Metabotropic glutamate receptors and glutamate transporters shape transmission at the developing retinogeniculate synapse. *J Neurophysiol*. 2013;109(1):113–123.
63. Rubel EW, Fritzsch B. Auditory system development: primary auditory neurons and their targets. *Annu Rev Neurosci*. 2002;25:51–101.
64. Harris JA, Rubel EW. Afferent regulation of neuron number in the cochlear nucleus: cellular and molecular analyses of a critical period. *Hear Res*. 2006; 21(6–217):127–137.
65. Lu Y. Endogenous mGluR activity suppresses GABAergic transmission in avian cochlear nucleus magnocellularis neurons. *J Neurophysiol*. 2007;97(2):1018–1029.
66. Tang ZQ, Liu YW, Shi W, et al. Activation of synaptic group II metabotropic glutamate receptors induces long-term depression at GABAergic synapses in CNS neurons. *J Neurosci*. 2013;33(40):15964–15977.
67. Chanda S, Oh S, Xu-Friedman MA. Calcium imaging of auditory nerve fiber terminals in the cochlear nucleus. *J Neurosci Methods*. 2011;195(1):24–29.
68. Chanda S, Xu-Friedman MA. Neuromodulation by GABA converts a relay into a coincidence detector. *J Neurophysiol*. 2010;104(4):2063–2074.
69. Brenowitz S, Trussell LO. Maturation of synaptic transmission at end-bulb synapses of the cochlear nucleus. *J Neurosci*. 2001;21(23):9487–9498.
70. Cook DL, Schwindt PC, Grande LA, Spain WJ. Synaptic depression in the localization of sound. *Nature*. 2003;421(6918):66–70.